Available online at www.sciencedirect.com
SCIENCE DIRECT®
Journal of Chromatography A, 1069 (2005) 91–97
JOURNAL OF CHROMATOGRAPHY A
www.elsevier.com/locate/chroma

Influence of particle diameter distribution on protein recovery in the expanded bed adsorption process

Krzysztof Kaczmarski[a,*], Jean-Christophe Bellot[b]

[a] *Department of Chemical Engineering, Faculty of Chemistry, Rzeszow University of Technology, ul. W. Pola 2, 35-959 Rzeszow, Poland*
[b] *Centre de Bioingénierie Gilbert Durand, UMR-CNRS 5504, UMR-INRA 792, INSA, 135 av. de Rangueil, 31077 Toulouse, Cedex 4, France*

Available online 10 November 2004

Abstract

The General Rate model has been developed and solved to describe protein adsorption in an expanded bed. The model takes into account axial and local variation of particle size distribution (PSD), external and intra-particle mass transfer resistances, and dispersion in liquid phase. The influence of PSD on breakthrough profiles has been analysed. The simulation results show that for a significantly high expanded bed the lower part of the breakthrough curve profiles, calculated for local particle size distribution (LPSD) and for axial average particle size distribution (APSD) are very similar. However, the upper part of breakthrough profiles calculated for LPSD approaches inlet concentration much more slowly than those calculated for APSD. The retention times of the lower part of uptake curves calculated with average particle diameter are constantly shorter than those obtained from LPSD. For the calculation of the dynamic capacity (DC), the LPSD can be replaced by APSD for large expanded bed heights. Using breakthrough profiles calculated for average particle size, DC values are constantly underestimated.

Keywords: Expanded bed adsorption; General Rate model; Mass transfer kinetics; Particle size distribution

1. Introduction

The production of proteins by using yeast or bacteria cells has become a very common technique for the preparation of pharmaceuticals. The feedstocks from which proteins are prepared are generally complex, containing solid and dissolved biomass of various sizes and molecular mass. One of the most efficient methods for protein separation from the cultivation broth is expanded bed adsorption (EBA) [1,2]. Highly efficient packed bed columns are not suitable for processing feedstocks with suspended biomass, as particles become trapped in the voids of the column bed. This results in the formation of a plug of trapped solids that finally leads to a complete blockage of the column. To avoid column blockage, the fluidized bed technique was adopted. The upper column adapter was removed and the mobile phase was pumped with such velocities as to attain typically a two-fold expansion of the bed in comparison with the settled bed height, thereby increasing interstitial bed voidage. To minimize axial dispersion, mono-disperse adsorbent particles are not generally used. The larger particles are located close to the bottom of the bed and the smaller particles are distributed towards the top. If particles have the appropriate size distribution, classification leads to layers of particles and reduced mixing in the column.

The EBA process is very long and frequently takes several hours. This is because experimental investigations of the influence of operating conditions and process parameters of protein recovery efficiency is very time consuming and expensive. Numerical models are therefore used to provide a fundamental understanding of the process and to establish optimum separation conditions.

One of the most sophisticated models, the General Rate model, has recently been used by Wright and Glasser [3] and Tong et al. [4] and Chen et al. [5] to interpret their ex-

* Corresponding author. Tel.: +48 17 865 1295; fax: +48 17 854 3655.
E-mail address: kkaczmarski@prz.rzeszow.pl (K. Kaczmarski).

0021-9673/$ – see front matter © 2004 Elsevier B.V. All rights reserved.
doi:10.1016/j.chroma.2004.09.077

perimental data and to carry out parametric analysis. In this model, mobile phase dispersion, solid phase dispersion, external and internal mass transfer resistances have been taken into account, but particle size distribution has been ignored.

As stated in the papers referred to above, a constant particle diameter has been assumed. However, particles with different sizes or with different sizes and different densities are used in the EBA process.

In a recent paper, Tong at al. [6] solved the EBA model while taking into account axial average particle size distribution (APSD), but still ignoring the axial bed porosity distribution.

In our previous paper [7], the more sophisticated EBA model was analyzed. The model takes into account all possible changes of parameters defined as a function of axial bed porosity distribution and axial particle size distribution. In addition, breakthrough profiles obtained for local particle size distribution identical with manufactured PSD (called below bulk particle size distribution—BPSD) were analyzed. Such particle size distributions were observed by Tong and Sun [8] for 6AS beads.

Simulations presented in [7] prove that the use of high settled beds is very efficient for the EBA process, which thus becomes less sensitive to experimental perturbations. These also confirm the conclusions already obtained previously with simpler models which state that dynamic capacity (DC) mainly depends on internal mass transfer resistances. The external mass transfer, axial liquid-phase dispersion and axial solid-phase dispersion have minor effects on DC. Moreover, it was proved that axial bed porosity distribution can be replaced by its average value with negligible errors.

For columns with BPSD, the slow approach of the plateau concentration for breakthrough profiles was observed. Finally, it has to be noted that previous authors, see Rasmuson [9] and recently Carta and Ubiera [10] have also studies the effects of particle-size distribution on the shape of breakthrough curves in packed beds. These works could be identified in their approach to what we have called the BPSD simulations i.e. an identical PSD regarding axial position. The work of Carta confirms that, with irreversible isotherms, BPSD simulations "yield breakthrough curves that approach saturation much more gradually than predicted using the average particle radius" [10].

However, for most adsorbents, the local particle size distribution (LPSD) is different at different column levels in EBA [8,11].

The aim of this work is the comparison of breakthrough profiles obtained for APSD, LPSD and for average particle diameter (APD). The results of this comparison provide answers to the problem as to if and when the APSD or APD can be used instead of LPSD for calculation of dynamic capacity. The replacement of LPSD by APSD or APD can noticeably reduce computation time because the EBA model with APSD or APD can be solved several hundred times faster than the model with LPSD.

2. Theory

2.1. Particle size distribution

For the widely used commercial adsorbent particles in EBA, such as Streamline particles, distribution of particle density is nearly uniform compared with that of particle size. Therefore, variations of particle densities in different column positions are ignored and only variations of particle size distribution will be considered here. The function of volume particle size distribution for Streamline particles is approximately expressed by normal Gaussian distribution [11]:

$$f_1(d) = \frac{1}{\sqrt{2\Pi}\sigma_s}\exp\left(-\frac{(d-d_p)^2}{2\sigma_s^2}\right) \quad (1)$$

where d_p and σ_s are the averaged diameter of the bulk adsorbent and standard deviation of the particles. Since there are no particles in the size range of $d\langle d_{min}$ or $d\rangle d_{max}$, Eq. (1) has been modified along the lines suggested by Yun et al. [11]:

$$f(d) = \frac{1}{1-\int_{-\infty}^{d_{min}} f_1(d)\delta d - \int_{d_{max}}^{\infty} f_1(d)\delta d}\frac{1}{\sqrt{2\Pi}\sigma_s} \times \exp\left(-\frac{(d-d_p)^2}{2\sigma_s^2}\right) \quad (2)$$

Eq. (2) fulfils the following condition:

$$\int_{d_{min}}^{d_{max}} f(d)\delta d = 1 \quad (3)$$

In this research, it has been assumed that function (2) can be used for calculation of PSD at each column level if the average particle diameter is replaced by axial average particle size distribution $d_p(x)$.

For Streamline particles, Tong and Sun [8] have found that the axial average particle size distribution can be expressed by the following equation:

$$d_p(x) = d_p(1.21 + 0.46X) \quad (4)$$

where $X = x/H$ is a dimensionless column length referenced to the expanded bed height, H.

The average particle size distribution expressed by Eq. (4) will from now on be referred to as axial particle size distribution.

After introduction of $d_p(x)$ into Eq. (1), the particle size distribution at each column level can be obtained. Calculated particle size distribution from Eq. (1) and (4) will be called local particle size distribution.

As an example, particle size distribution for different X values, is presented in Fig. 1. The calculations were carried out for mean particle diameter $d_p = 210\,\mu m$ and constant value of standard deviation $\sigma_s = 62\,\mu m$. From experimental data presented in [8,11] it follows that standard deviation decreases along column height by a fac-

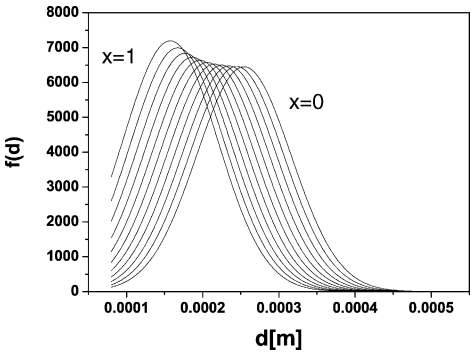

Fig. 1. The particle size distribution calculated from Eqs. (2) and (4) for $X = 0, 0.1, 0.2, \ldots, 0.9, 1$. The mean particle diameter was $d_p = 210\ \mu m$ and standard deviation $\sigma_s = 62\ \mu m$.

tor of roughly two. However, in this work, we have ignored this dependency because of unknown relationship between standard deviation and distance from the column bottom.

The calculated LPSD is not exactly the same as experimental distribution [8,11], however it can be used to predict qualitative differences between breakthrough profiles calculated for APD, APSD and LPSD.

To simulate breakthrough curve profiles with LPSD, the column was divided into 10 equally spaced sectors. The average particle diameter was calculated from Eq. (4) for each sector. Inside the sector the particle size distribution was approximated by discrete distribution. The interval between d_{max} and d_{min} was divided into 20 fractions. The value of discrete density distribution for each fraction was calculated from integral:

$$\bar{f}(d_{a,i}) = \int_{d_i}^{d_i+\Delta d} f(d)\delta d \tag{5}$$

where

$$\Delta d = \frac{(d_{max} - d_{min})}{20} \tag{6}$$

and

$$d_{a,i} = d_i + \frac{\Delta d}{2} \tag{7}$$

2.2. EBA model

For the investigation of the impact of local particle size distribution on breakthrough profiles, the bed voidage distribution along the column and the solid phase dispersion were neglected because of their minor influence on concentration band profiles [7].

With the above assumptions the EBA model consists of two differential mass transport equations:

- the mass transport equation for the species in the mobile fluid phase:

$$\varepsilon_e \frac{\partial C}{\partial t} + u\frac{\partial C}{\partial x} = \varepsilon_e D_L \frac{\partial^2 C}{\partial x^2} - \sum_i \times \left(\frac{(1-\varepsilon_e)\times \bar{f}(d_{a,i}) \times 3 \times k_{ext,i}(C - C_{p,i}(r = R_i))}{R_i} \right) \tag{8}$$

initial condition

for $t = 0$

$$C(x, 0) = 0 \tag{9}$$

boundary conditions

for $x = 0$

$$C = C_o + \frac{D_L \varepsilon_e}{u}\frac{\partial C}{\partial x} \tag{10}$$

for $x = H$

$$\frac{\partial C}{\partial x} = 0 \tag{11}$$

- the mass transport equation for particle:

$$\varepsilon_p \frac{\partial C_{p,i}}{\partial t} + \frac{\partial q}{\partial t} = \frac{D_m \varepsilon_p}{\theta}\frac{1}{r^2}\frac{\partial}{\partial r}\left(r^2 \frac{\partial C_{p,i}}{\partial r}\right) \tag{12}$$

initial condition

for $t = 0$

$$q(x, r, 0) = 0, \qquad C_p(x, r, 0) = 0 \tag{13}$$

boundary conditions

for $r = 0$

$$\frac{\partial C_p}{\partial r} = 0 \tag{14}$$

for $r = R_i$

$$\frac{\varepsilon_p D_m}{\theta}\frac{\partial C_{p,i}}{\partial r} = k_{ext,i}(x) \times (C - C_{p,i}) \tag{15}$$

In above equations, C and C_p (mg species/ml of fluid) are the concentrations of the solute in the percolating stream and in the stagnant liquid phase, respectively. C_o is the inlet concentration, q (mg species/ml of adsorbent) is the adsorbate concentration, x is the distance along the column, t is the time, r is the distance from the particle center, $R_i = d_{a,i}/2$ is the particle radius, H is the expanded bed height, ε_e is the bed (external) porosity, ε_p the internal or mesopore porosity, u is the superficial velocity, D_L is the mobile phase axial dispersion coefficients, D_m is the molecular diffusivity, k_{ext} is the mass transfer coefficient from bulk phase to the external surface of the particle and finally θ is the pore tortuosity. The index i denotes the ith fraction of particle diameter distribution—see point 2.1.

Table 1
Calculated dispersion coefficients D_L from experimental values of Bodenstein number (Bo) [14] The column diameter $D = 0.05$ m, superficial velocity $u = 0.0006167$ m/s and voidage $\varepsilon_e = 0.64$

Settled matrix height H_0 (cm)	Expanded bed height H (cm)	H/H_0	Bo = $u \times H/(D_L \cdot \varepsilon_e)$	$D_L \times 10^6$ (m^2/s, calculated)
10.18	19.4	1.90	29.2	6.40
12.73	24.2	1.90	28.6	8.15
14.00	26.8	1.91	36.7	7.04
15.28	29	1.90	36.8	7.59
17.82	34.3	1.92	40.6	8.14
19.10	36.2	1.89	37	9.43
20.37	40	1.96	42.8	9.00
30.56	58.5	1.91	45.5	12.4
38.20	73.3	1.92	49.2	14.3

In the case of APSD the sum in Eq. (8) is replaced by the term:

$$\frac{(1-\varepsilon_e) \times 6 \times k_{ext}(C - C_p(r=R))}{d_p(x)} \tag{16}$$

where $d_p(x)$ is calculated from Eq. (4).

When calculations are performed for APD, the axial diameter distribution, $d_p(x)$, is replaced by average particle diameter.

2.3. EBA model parameters value

The EBA model was solved with Langmuir isotherm. This isotherm is frequently used to describe adsorption of proteins [4,12]:

$$q = \frac{q_m \times C}{K_d + C} \tag{17}$$

where q_m is the maximum adsorption capacity and K_d is the dissociation constant.

In the following $q_m = 50$ mg/ml and $K_d = 0.1$ mg/ml were assumed.

The mass transfer coefficient characterizing mass transfer from bulk phase to external particle surface, k_{ext}, was calculated from the Carberry correlation, as recommended by Hunter and Carta [12]. The correlation for each ith fraction of particles can be written as follows:

$$k_{ext,i}(x) = 1.15\frac{u}{\varepsilon_e}\left(\frac{u \times d_{a,i} \times \rho}{\eta}\right)^{-1/2}\left(\frac{\eta}{\rho D_{AB}}\right)^{-2/3} \tag{18}$$

The value of the binary diffusion coefficient, D_{AB}, was taken as for BSA, equal to 5.3×10^{-11} m^2/s [13]. For calculation of k_{ext}, the following parameters were assumed: density, $\rho = 1000$ kg/m^3, viscosity, $\eta = 0.001$ kg/m/s, superficial velocity $u = 0.0006167$ m/s. Other model parameters were assumed as follow: pore diffusivity $D_m/\theta = D_p = 3e\text{-}11$ m^2/s, average bed porosity $\varepsilon_e = 0.7$, particle porosity $\varepsilon_p = 0.5$ and inlet concentration C_o was equal 0.5 mg/ml

One of the problems in modeling EBA processes is the lack of an appropriate correlation for the mobile phase axial dispersion coefficient. To simulate breakthrough peak profiles, we decided to use mean values of experimental axial dispersion coefficients for given expanded bed height measured by Thömmes et al. [14]. The data used by Thömmes et al. in [14] are given in Table 1.

The values of model parameters assumed in this work are summarized in Table 2.

The discussed above EBA model was solved using orthogonal collocation on finite element method [15,16].

3. Results and discussion

The simulation of breakthrough profiles was carried out for particle size distribution given by Eqs. (2) and (4). The calculations were made for three sets of parameter values for the particle size distribution model given by Eq. (2).

(a) $d_{min} = 80$ μm; $d_{max} = 500$ μm; bulk mean diameter, $d_p = 210$ μm; and $\sigma_s = 62$ μm
(b) $d_{min} = 38$ μm; $d_{max} = 238$ μm; bulk mean diameter $d_p = 100$ μm; and $\sigma_s = 29.5$[μm]
(c) $d_{min} = 19$ μm; $d_{max} = 119$ μm; bulk mean diameter, $d_p = 50$ μm; and $\sigma_s = 14.8$ μm

In the case (a), the value of PSD parameters are the experimental data for Streamline particles [11]. For purposes of comparison, we have also performed calculations for two fictitious distributions (b and c).

Table 2
The values of model parameters

Name	Value
C_o (mg/ml), inlet concentration	0.5
d_p (μm), average particle diameter	50, 100, 210
Average axial particle diameter distribution	Eq. (4)
Local particle size distribution	Eq. (2)
D_{AB} (m^2/s), binary diffusion coefficient	5.3×10^{-11}
D_s (m^2/s), solid phase dispersion coefficient	6.7×10^{-8}
D_p (m^2/s), pore diffusivity	3e-11
K_d (mg/ml), maximum adsorption capacity	0.1
q_m (mg/ml), dissociation constant	50
u (m/s), superficial velocity	0.0006167
ε_e, average bed porosity	0.7
ε_p, particle porosity	0.5
ρ (kg/m^3), density	1000
η (kg/m/s), mobile phase viscosity	0.001
Bed height and liquid phase dispersion coefficient	Table 1

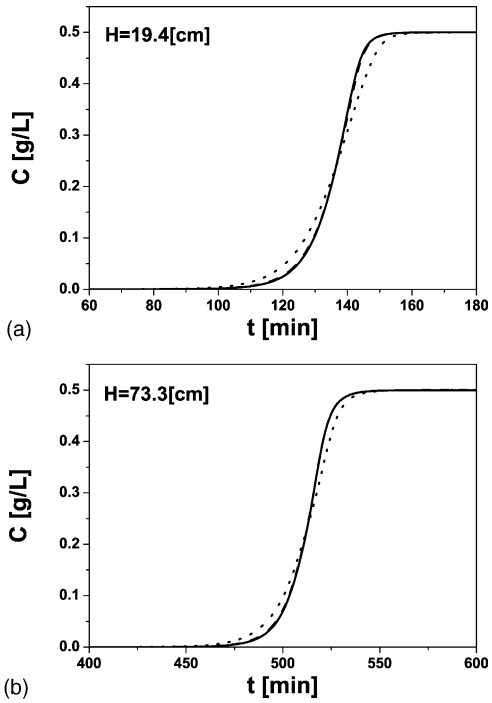

Fig. 2. (a) Comparison of concentration profiles calculated for an average particle diameter equal to 50 μm. Solid line represents calculation for LPSD, dashed line, calculation for APSD and doted line, calculation for average particle diameter. (b) Comparison of concentration profiles calculated for average particle diameter equal to 50 μm. Legend is the same as for Fig. 2a.

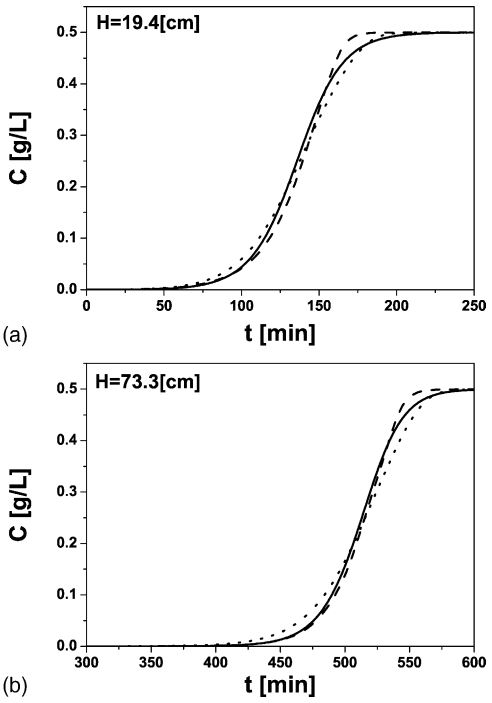

Fig. 3. (a) Comparison of concentration profiles calculated for average particle diameter equal to 100 μm. Legend is the same as for Fig. 2a. (b) Comparison of concentration profiles calculated for average particle diameter equal to 100 μm. Legend is the same as for Fig. 2a.

In Fig. 2a and b the comparison of concentration profiles calculated for LPSD, APSD and for average particle diameter is presented. The average particle diameter was equal to 50 μm. The simulations were performed for expanded bed height, H, equal to 18.4 and 73.3 cm. In Fig. 3a and b and Fig. 4a and b similar calculations for average particle diameter equal to 100 and 210 μm, respectively are presented. From a comparison of breakthrough profiles calculated for LPSD and APSD it follows that:

- the band profiles overlap each other for the smallest average particle diameter,
- for $H = 73.3$ cm and for any average particle diameter, the lower part of breakthrough profiles are very similar,
- differences between band profiles are observed for the upper part of uptake curves and average particle diameters equal to 100 and 210 μm. The profiles obtained by considering LPSD, approach the plateau concentration much more slowly than the one obtained for APSD. This theoretical prediction is in qualitative agreement with experimentally observed concentrations very slowly approaching the plateau, as for instance in the case of adsorption of BSA on BRX-Q, DEAE Spherodex M and Streamline DEAE column [5,6,10]. The local particle size distribution may be in some degree responsible for the tailing behavior. However, the tailing can be also caused by BSA dimmer presented in BSA sample [12]. In the case of EBA processes, the most important is a precise determination of breakthrough pro-

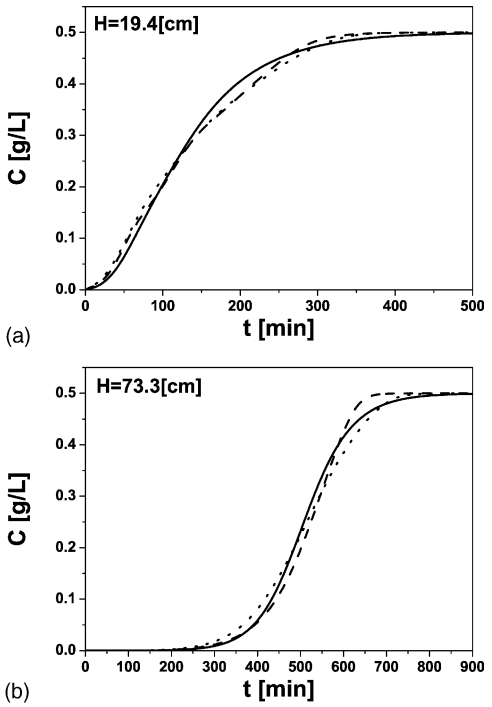

Fig. 4. (a) Comparison of concentration profiles calculated for average particle diameter equal to 210 μm. Legend is the same as for Fig. 2a. (b) Comparison of concentration profiles calculated for average particle diameter equal to 210 μm. Legend is the same as for Fig. 2a.

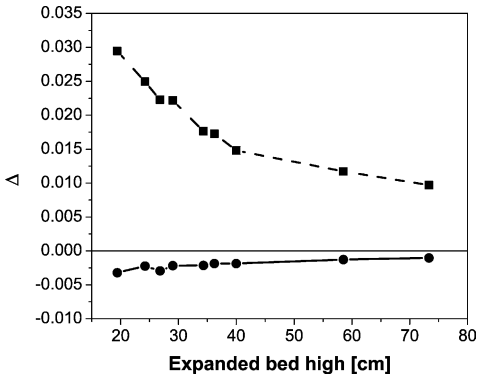

Fig. 5. Dependency on relative retention time differences for $C = 0.1C_o$ on expanded bed height. Average particle diameter is equal to 50 μm. The solid line represents the Δ_{APSD}, the dashed line the Δ_t.

files for concentrations up to $0.1C_o$ because the calculation of dynamic capacity is recommended [17] for that concentration value. From presented simulations, it is evident that the retention time for outlet concentration equals to $0.1C_o$ is always smallest when read from band profiles calculated for average particle diameter. The estimated value of DC would be in such case underestimated.

In Figs. 5 and 6 the dependency of relative retention time differences, Δ_t or Δ_{APSD}, on expanded bed height are presented.

The parameter Δ is defined as follows:

$$\Delta_t = \frac{t_{LPSD} - t}{t_{LPSD}} \text{ or } \Delta_{APSD} = \frac{t_{LPSD} - t_{APSD}}{t_{LPSD}} \quad (19)$$

where t_{LPSD}, t_{APSD} and t are the retention times for outlet concentration equal to $0.1C_o$ for breakthrough profiles calculated when LPSD, APSD or APD respectively were assumed.

The relative retention time differences always decrease with increasing expanded bed height. For average particle diameter equal to 50 μm the value of Δ_t is less than 3% and value of $|\Delta_{APSD}|$ is less than 0.3%. For average particle diameter equal to 100 μm the following relations hold:

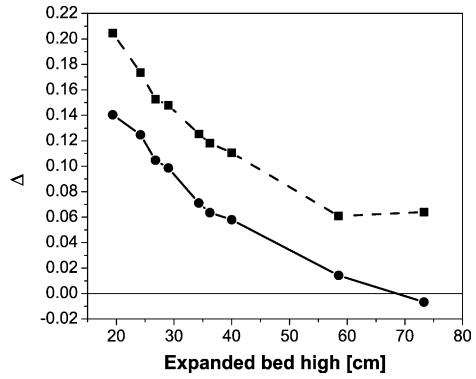

Fig. 6. Dependency on relative retention time differences for $C = 0.1C_o$ on expanded bed height. Average particle diameter is equal to 210 μm. The solid line represents the Δ_{APSD}, the dashed line the Δ_t.

$\Delta_t < 6\%$, $|\Delta_{APSD}| < 2\%$ (figure not presented). Much larger relative retention time differences are for average particle diameter equal to 210 μm. Only for expanded bed larger than 50 cm the $|\Delta_{APSD}|$ is less than about 3%. The Δ_t decreases from about 20% to 6%.

From the comparison presented, it follows that for precise calculations of DC, the APSD can be used instead of LPSD for relatively small particle diameters or large expanded bed height. This conclusion is important from the point of view of EBA process optimization. Solution times investigated here were from several to 90 s on PC Athlon 2.2 GHz computer when APSD or average particle diameter was used for simulation. The simulation concerning LPSD took from about 4 h to 1 day.

4. Conclusions

In this work, the EBA breakthrough profiles calculated for local and axial particle size distributions were compared with band profiles obtained for average particle diameter. The elaborated program can be used for any local particle size distribution, however, because of the illustrative purpose of this work, we restricted our investigation to Gaussian like distribution.

From the analysis of the lower part of breakthrough profiles, it is evident that simulations performed for APSD constantly approximate a much better concentration band obtained for LPSD in comparison with solutions for APD. The differences between relative retention times, Δ_{APSD}, for outlet concentration equals to $0.1C_o$, for which the dynamic capacity is calculated, are negligible when the average particle diameter is less than 100 μm or the expanded bed height is large. In these cases the LPSD can be replaced by APSD that gives the possibility of rapidly optimizing the EBA process.

Acknowledgement

This work was supported by Grant 4 T09C 00623 of the Polish State Committee for Scientific Research.

References

[1] J. Thommes, Adv. Biochem. Eng. 58 (1997) 185.
[2] H.A. Chase, Trends Biotechnol. 12 (1994) 296.
[3] P.R. Wright, B.J. Glasser, AIChE J. 47 (2001) 474.
[4] X.-D. Tong, X.-Y. Dong, Y. Sun, Biochem. Eng. J. 12 (2002) 117.
[5] W.-D. Chen, X.-D. Tong, X.-Y. Dong, Y. Sun, Biotechnol. Prog. 19 (2003) 880.
[6] X.-D. Tong, B. Xue, Y. Sun, Biochem. Eng. J. 16 (2003) 265.
[7] K. Kaczmarski, J.-Ch. Bellot, Biotechnol. Prog. 20 (2004) 786.
[8] X.-D. Tong, Y. Sun, J. Chromatogr. A 977 (2002) 173.
[9] A. Rasmuson, Chem. Eng. Sci. 40 (1985) 621.
[10] G. Carta, A. Ubiera, AIChE J. 49 (2003) 3066.

[11] J. Yun, S.-J. Yao, D.-Q. Lin, M.-H. Lu, W.-T. Zhao, Chem. Eng. Sci. 59 (2004) 449.
[12] A.K. Hunter, G.J. Carta, J. Chromatogr. A 897 (2000) 81.
[13] M.T. Tyn, T.M. Gusek, Biotechnol. Bioeng. 35 (1990) 327.
[14] J. Thommes, M. Weiher, A. Karau, M.R. Kula, Biotechnol. Bioeng. 48 (1995) 367.
[15] V.J. Villadsen, M.L. Michelsen, Solution of Differential Equation Model by Polynomial Approximation, Prentice Hall, Englewood Cliffs, NJ, 1978.
[16] K. Kaczmarski, D. Antos, H. Sajonz, P. Sajonz, G.J. Guiochon, J. Chromatogr. A 925 (2001) 1.
[17] L.J. Bruce, H.A. Chase, Chem. Eng. Sci. 56 (2001) 3149.